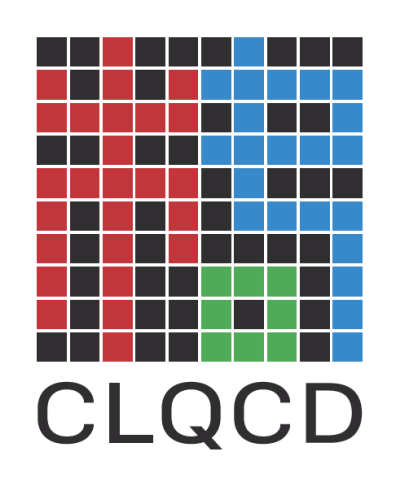
# Accurate nucleon iso-vector scalar and tensor charge at physical point

Speaker: JI-Hao Wang

Institute of Theoretical Physics, Chinese Academy of Sciences





#### Introduction

The nucleon iso-vector scalar and tensor charges,  $g_S$  and  $g_T$ , are fundamental quantities for characterizing nucleon structure. They can be used to:

- > determine the proton-neutron mass difference,
- constrain parton distribution functions,
- probe possible scalar and tensor interactions beyond the Standard Model
- **>** ..

They can only be reliably computed from first principles using lattice QCD, but precise calculations are challenging due to excited-state contamination and increased statistical noise at large time separations.

In this work, we use the **blending method** [1] and **current-inspired interpolating fields** [2,3] toreduce statistical errors and better control excited-state effects.

<sup>[1].</sup> Z.-C. Hu, J.-H. Wang, X. Jiang, L. Liu, S.-H. Su, P. Sun, and Y.-B. Yang, (2025), arXiv:2505.01719 [hep-lat].

<sup>[2].</sup> L. Barca, G. Bali, and S. Collins, Phys. Rev. D 111,L031505 (2025), arXiv:2412.13138 [hep-lat].

<sup>[3].</sup> L. Barca, (2025), arXiv:2508.09006 [hep-lat].

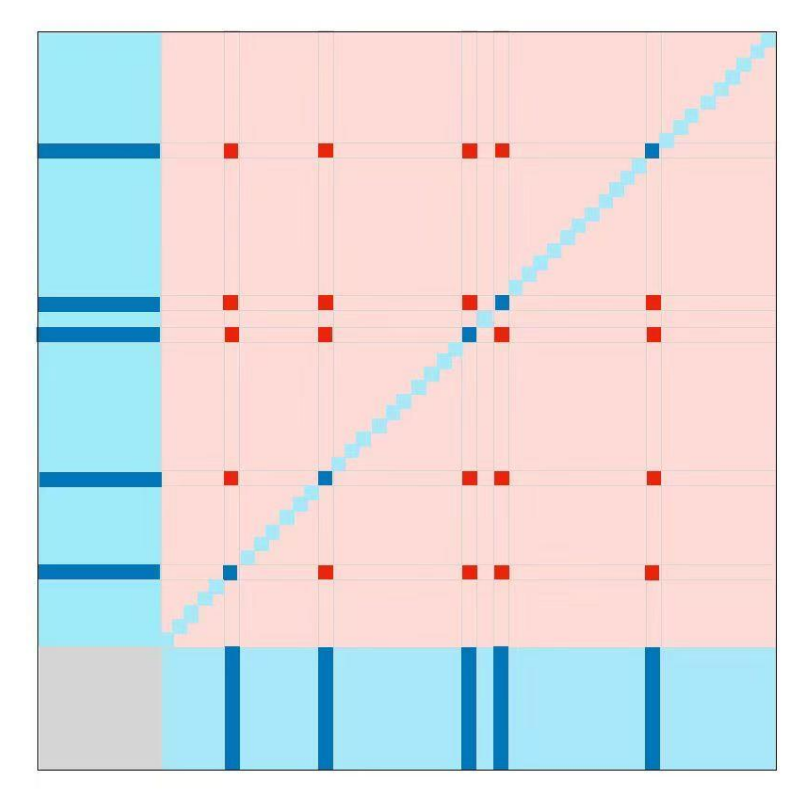
# Blending method

The blending method provides an approach to calculate matrix elements within the distillation framework.

- $\blacktriangleright$  In the distillation, only the information from  $\mathcal{L}_1$  is used to approximate the all-to-all propagator.
- ightharpoonup In the blending, full information from  $\mathcal L$  is recovered through random sampling in  $\mathcal L_2$  .

#### definition:

- $\succ$   $\mathcal{L}$ : the vector space associated with the lattice sites and color degrees of freedom
- $ightharpoonup \mathcal{L}_1$ : The span of  $N_e$  low-lying eigenvectors of the discrete Laplace operator
- $\triangleright \mathcal{L}_2$ : The orthogonal complement of  $\mathcal{L}_1$  in  $\mathcal{L}$



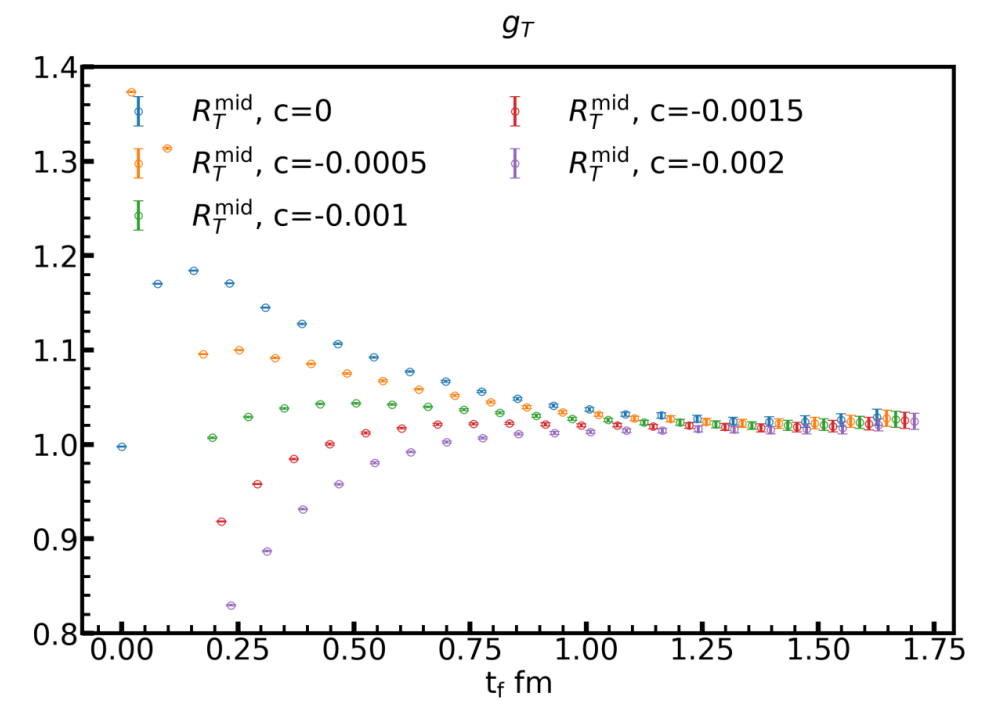
$$\Omega_{ij}^{(2)} = \begin{cases} 1 & \text{for } i,j \leq N_{\text{e}}, \\ \frac{\prod_{i=0}^{1} \frac{V - N_{\text{e}} - i}{N_{\text{st}} - i}}{N_{\text{st}} - i} & \text{for } i,j > N_{\text{e}}, \ i \neq j \\ \frac{V - N_{\text{e}}}{N_{\text{st}}} & \text{for the other cases,} \end{cases}$$

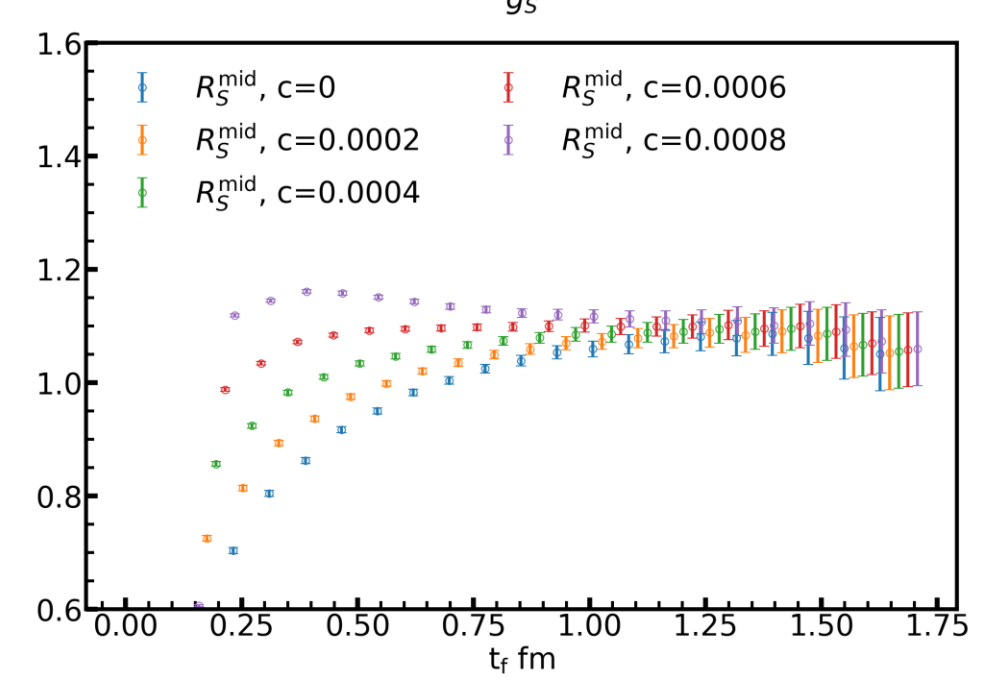
# Current inspired interpolating fields

For a given current operator  $O_X$ , the current-inspired interpolation field is  $NO_X$ , where  $N \equiv \epsilon_{abc} (u_a^T C \gamma_5 d_b) u_c$  and  $O_X = \overline{u} \Gamma_X u - \overline{d} \Gamma_X d$  with  $\Gamma_S = \mathbb{I}$  and  $\Gamma_T = \sigma_{uv}$ .

The ratio of  $N + cNO_X$  with different coefficient c on F48P30

$$\mathcal{R}_{X}(t_{f}, t; \mathcal{N}) = \frac{\int d^{3}x d^{3}y d^{3}z \langle \mathcal{N}(\vec{x}, t_{f}) \mathcal{O}_{X}(\vec{y}, t) \mathcal{N}^{\dagger}(\vec{z}, 0) \rangle}{\int d^{3}x d^{3}z \langle \mathcal{N}(\vec{x}, t_{f}) \mathcal{N}^{\dagger}(\vec{z}, 0) \rangle}$$
$$\mathcal{R}_{X}^{\text{mid}} \equiv \mathcal{R}_{X}(t_{f}, t_{f}/2)$$

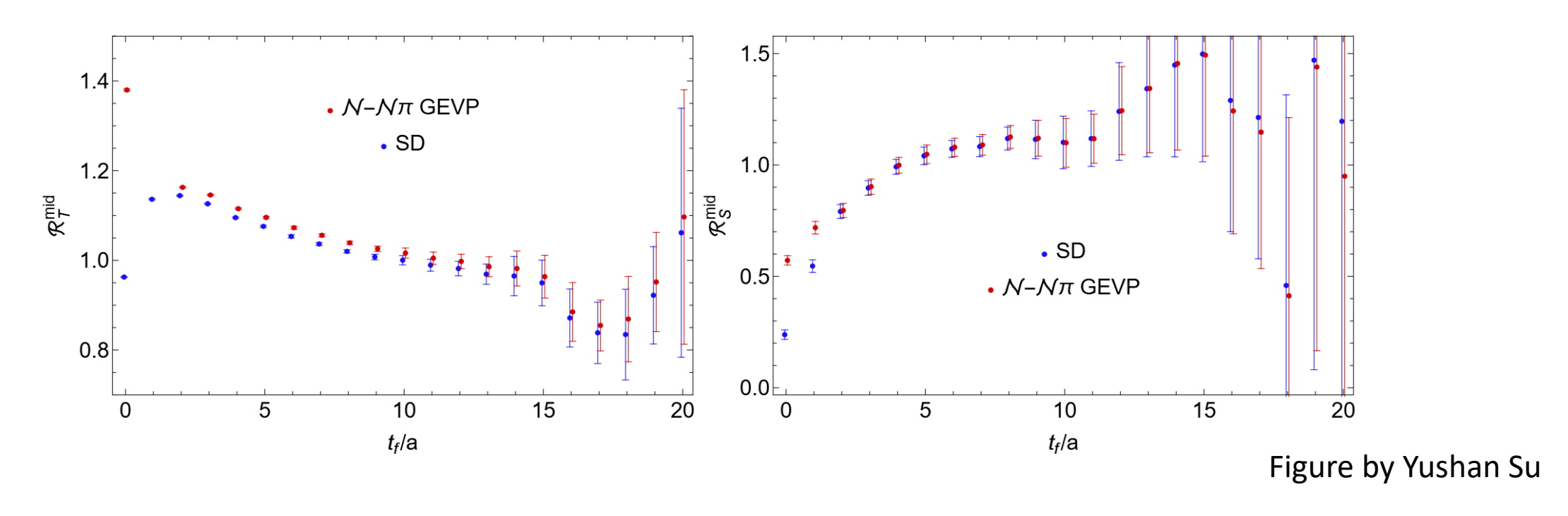




Since the disconnect part of  $NO_X$  to N 3pt is proportional to the volume, the small coefficient needed.

current-inspired interpolation fields are dominate the excited-state contamination

#### excited state $N\pi$

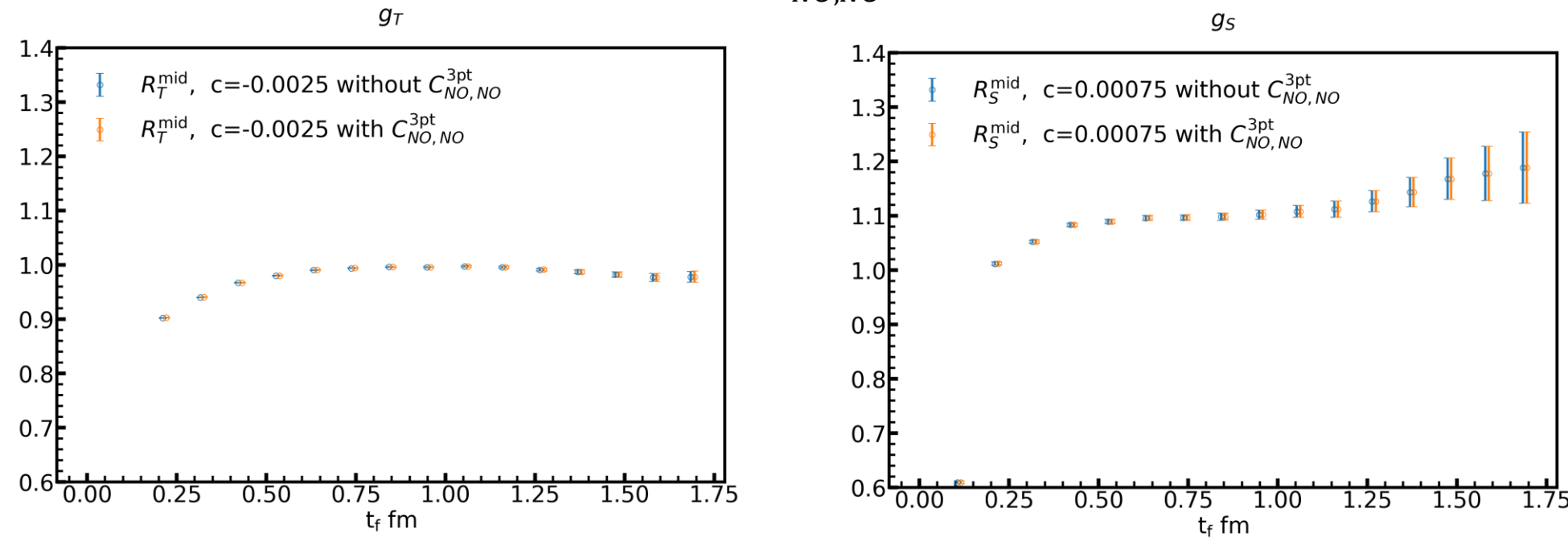


The contribution of  $N\pi$  to the excited state contamination is not significant.

# The contribution of $C_{NO,NO}^{3pt}$

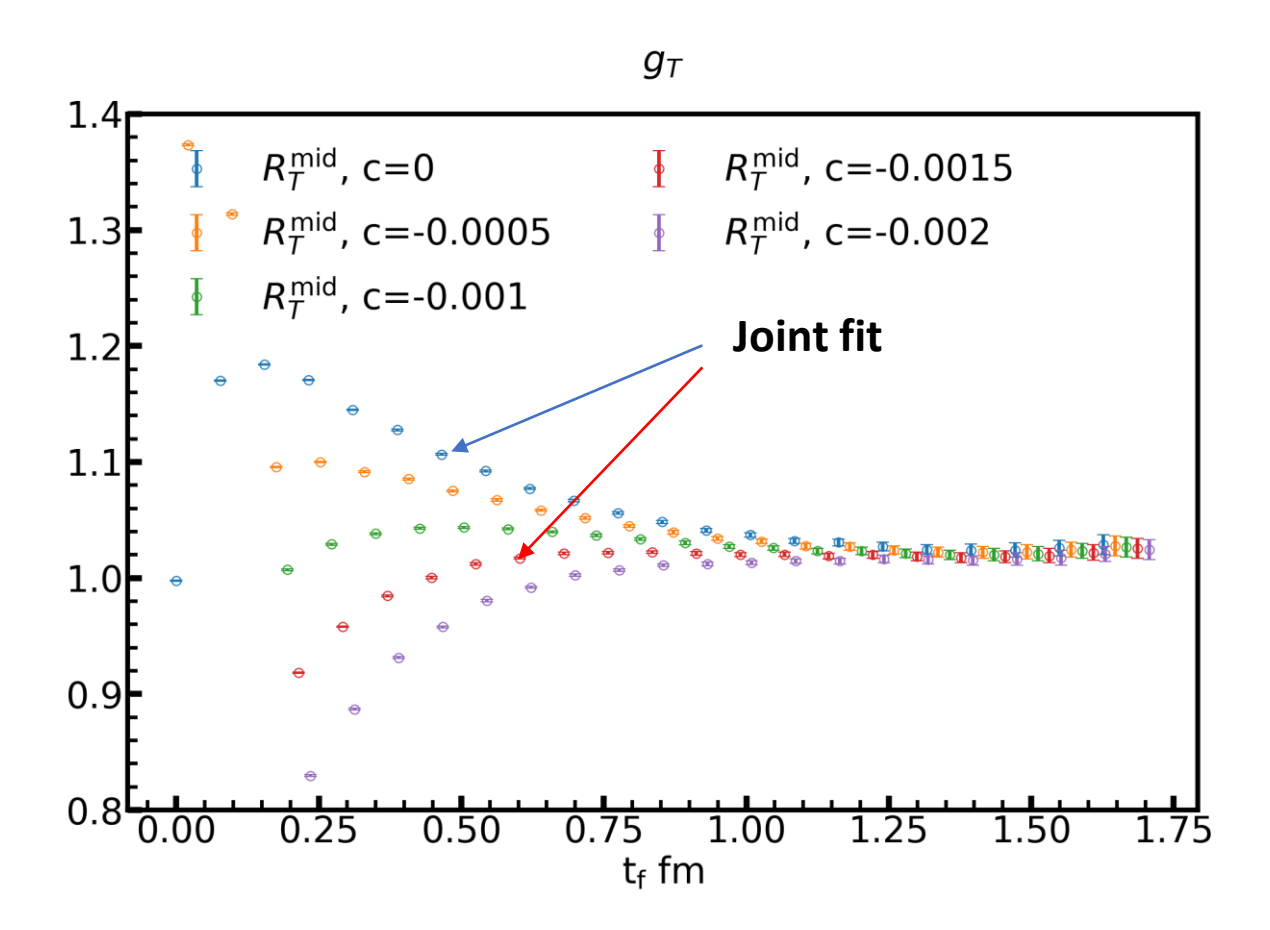
The  $C_{NO,NO}^{3pt}$  need calculate 26 diagrams and the  $C_{NO,NO}^{3pt}$  need calculate 138 diagrams

#### The contribution of $C_{NO,NO}^{3pt}$ on C32P29



The contribution  $C_{NO,NO}^{3pt}$  is very small due to the small coefficient c. Therefore, to save computing resources, we calculate  $C_{NO,NO}^{3pt}$  only for ensembles with  $N_e < 100$ 

# Fitting methodology



Choose c=0 and optimized coefficient c =  $c_X$  with mild time-dependences  $R_X^{\rm mid}(t_f)$  to do the joint fit

$$\begin{split} c_2(t_f;c) &= [1 + d_1^2(c)e^{-\Delta_1 t_f} + d_2^2(c)e^{-\Delta_2 t_f}]Z(c)e^{-E_0 t_f}, \\ \mathcal{R}_X(t_f,\,t;c) &= [b_{00} + b_{10}d_1(c)(e^{-\Delta_1 t} + e^{-\Delta_1(t_f-t)}) + b_{20}d_2(c)(e^{-\Delta_2 t} + e^{-\Delta_2(t_f-t)}) \\ &+ b_{11}d_1^2(c)e^{-\Delta_1 t_f} + b_{12}d_1(c)d_2(c)(e^{-\Delta_1(t_f-t)-\Delta_2 t} + e^{-\Delta_2(t_f-t)-\Delta_1 t}) + b_{22}d_2^2(c)e^{-\Delta_2 t_f}] \\ / [1 + d_1^2(c)e^{-\Delta_1 t_f} + d_2^2(c)e^{-\Delta_2 t_f}] \;, \end{split}$$

# Simulation Setup

We do the calculation on these ensembles

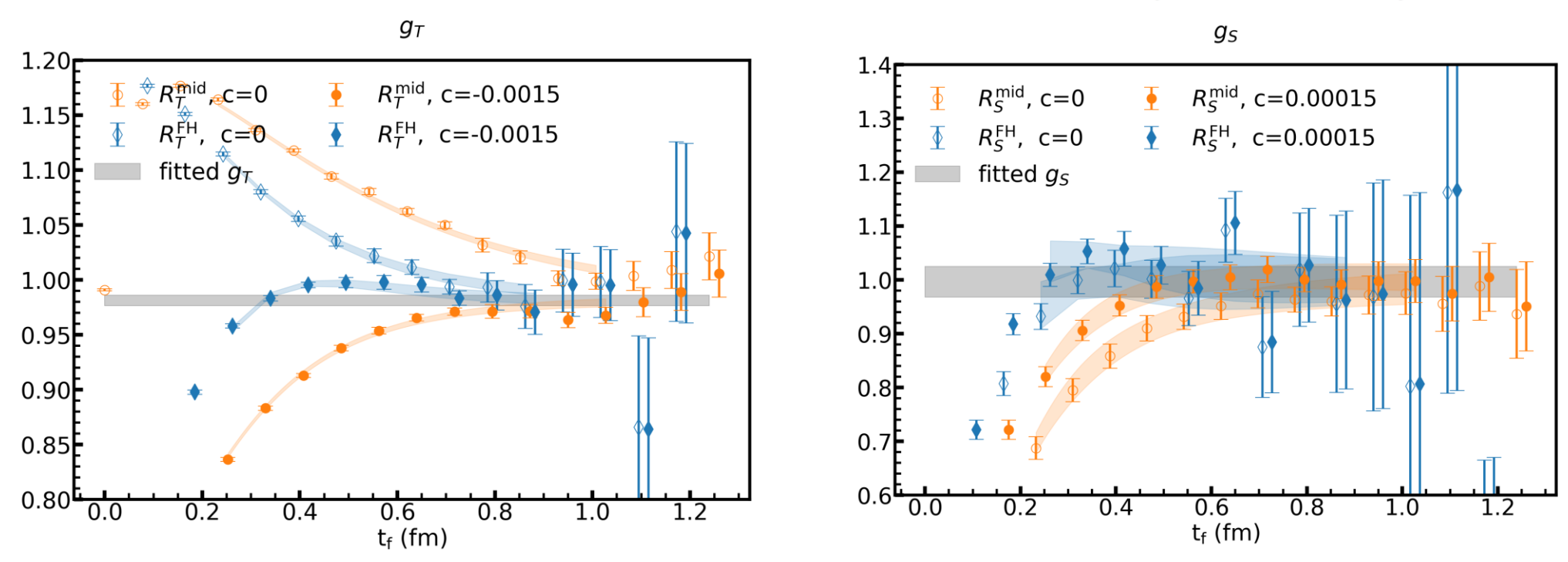
	$a(\mathrm{fm})$	$n_L^3 \times n_T$	$m_{\pi}(\mathrm{MeV})$	$m_{\pi}L$	$m_{\eta_s}({ m MeV})$	$n_{ m cfg}$
C24P34	0.1053	24x64	341.1(1.8)	4.38	748.61(75)	48
C24P29		24x72	292.7(1.2)	3.75	657.83(64)	96
C32P29		32x64	292.4(1.1)	5.01	658.80(43)	176
C24P23		24x64		2.93		71
C32P23		32x64	228.0(1.2)	3.91	643.93(45)	81
C48P23		48x96	225.6(0.9)	5.79	644.08(62)	54
C48P14		48x96	135.5(1.6)	3.81	706.55(39)	46
C64P14		64x128	134.5(1.6)	4.63	706.55(39)	40
E32P29	0.08973	32x64	288.1	4.19	705.6	99
F32P30	0.07753	32x96	303.2(1.3)	3.56	675.98(97)	91
F48P30		48x96	303.4(0.9)	5.72	674.76(58)	40
F32P21		32x64	210.9(2.2)	2.67	658.79(94)	300
F48P21		48x96	207.2(1.1)	3.91	661.94(64)	61
F64P13		64x128	134.1(1.5)	3.37	681.48(59)	40
G36P29	0.06887	36x108	297.2	3.73	693.05(46)	43
H48P32	0.05199	48x144	317.2(0.9)	4.00	691.88(65)	46

We use three ensembles with physical pion masses, spanning two different lattice spacings and two different volumes. This allows us to better control uncertainties at the physical point.

# Results on physical point

The results on F64P13(a=0.074fm,  $m_\pi=131$ MeV)

$$\mathcal{R}_X^{\mathrm{FH}}(t_f) \equiv \sum_{t=t_c}^{t_f+a-t_c} \mathcal{R}_X(t_f+a,t) - \sum_{t=t_c}^{t_f-t_c} \mathcal{R}_X(t_f,t) = \langle \mathcal{O}_X \rangle_N + \mathcal{O}(e^{-\delta m t_f}),$$



we achieve results with very small statistical errors on ensembles with physical pion masses!

## Cost comparison

#### The comparison of costs at the physical point for different collaborations

	Ensembles	L	Т	a(fm)	$m_\pi$ (MeV)	$n_{ m cfg}$	$g_T^{u-d}$	Propagators	Propagators for 1% error
CLQCD	F64P13	64	128	0.074	134	40	0.98(01)	0.34M	0.08M
ETMC	cB211.072.64	64	128	0.080	139	750	0.94(03)	1.71M	12.5M
RQCD	D452	64	128	0.076	156	1000	0.86(11)	0.01M	1.2M
PNDME	a09m130	64	96	0.090	138	1290	0.96(02)	1.69M	8.1M

Our method is significantly more efficient than traditional approaches and also offers better control of excited-state contamination by providing more information across different source—sink separations and nucleon interpolating fields.

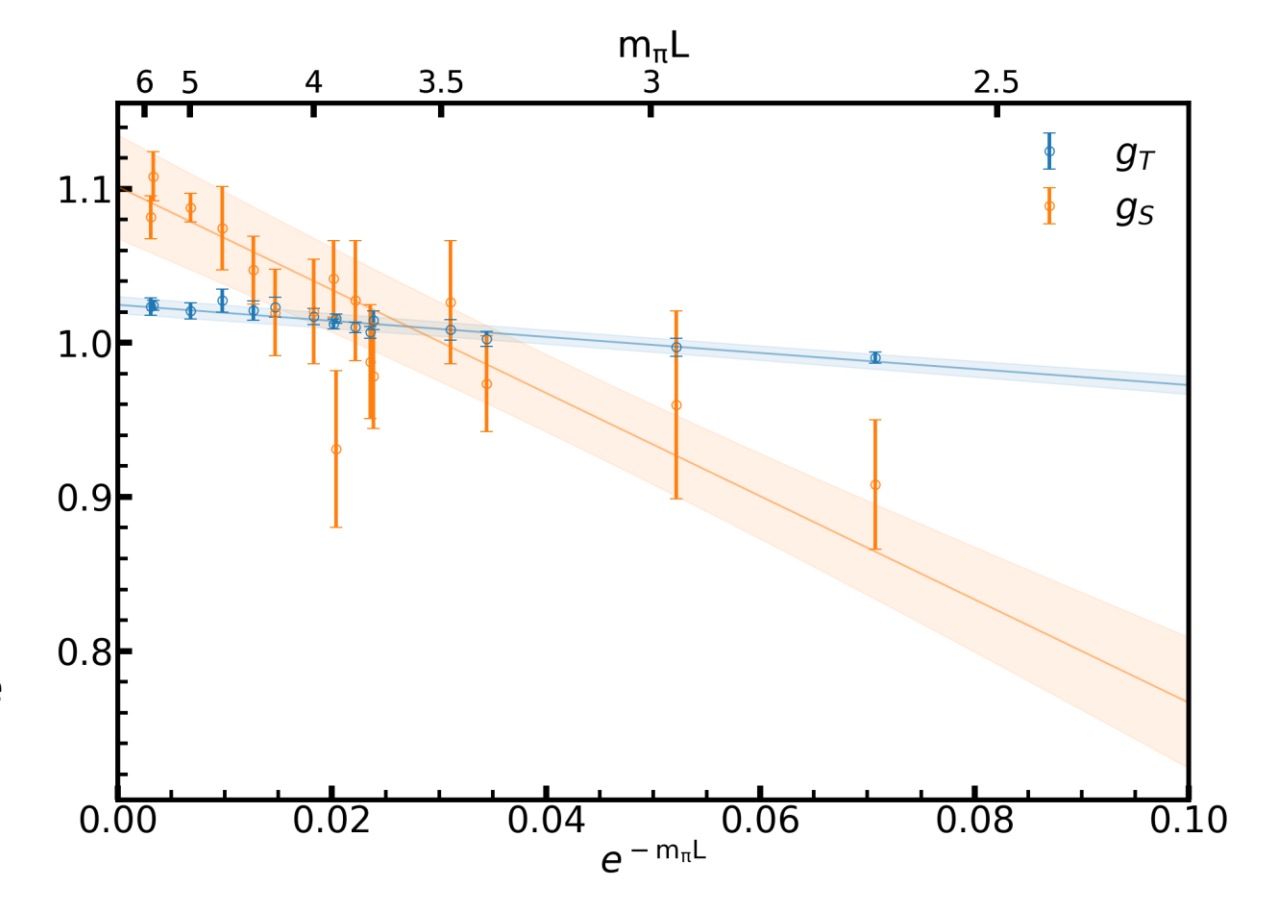
#### Finite volume effect

Global fit ansatz:

$$g_X(a, m_{\pi}, L) = g_X^{\text{QCD}} \left( 1 + \sum_{i=2,3} c_l^{(i)} (m_{\pi}^i - m_{\pi, \text{phy}}^i)) \right)$$
$$(1 + c_V e^{-m_{\pi} L}) + c_a^{(1)} a^2,$$

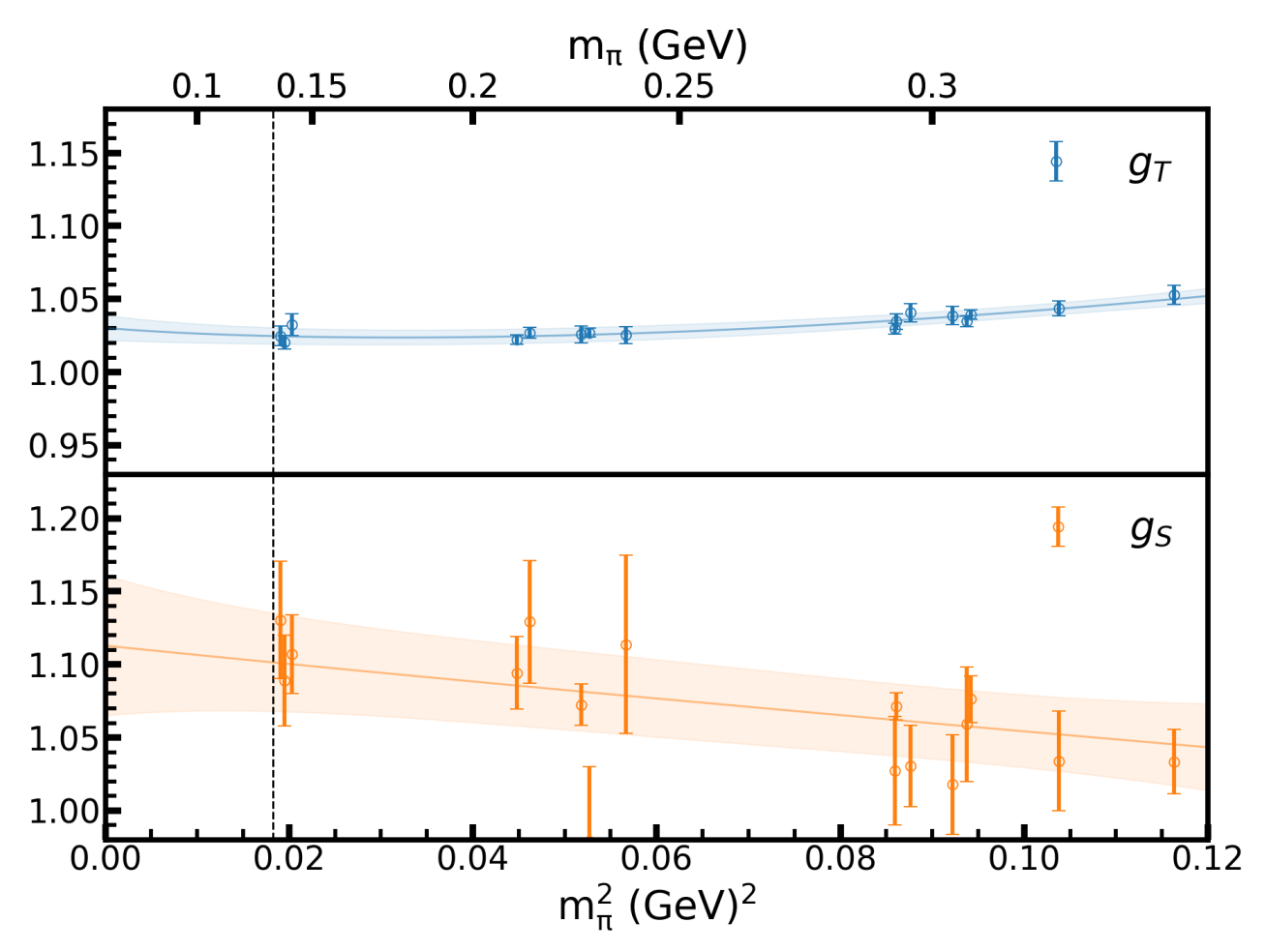
where  $g_X^{
m QCD}$  is the target physical value.

Our data strongly prefer the form  $e^{-m_\pi L}$  for finite-volume effects over the form  $m_\pi^2 e^{-m_\pi L}/\sqrt{m_\pi L}$  predicted by heavy baryon chiral perturbation theory (HB $\chi$ PT)



All data point have been corrected to continuum limit and physical pion mass

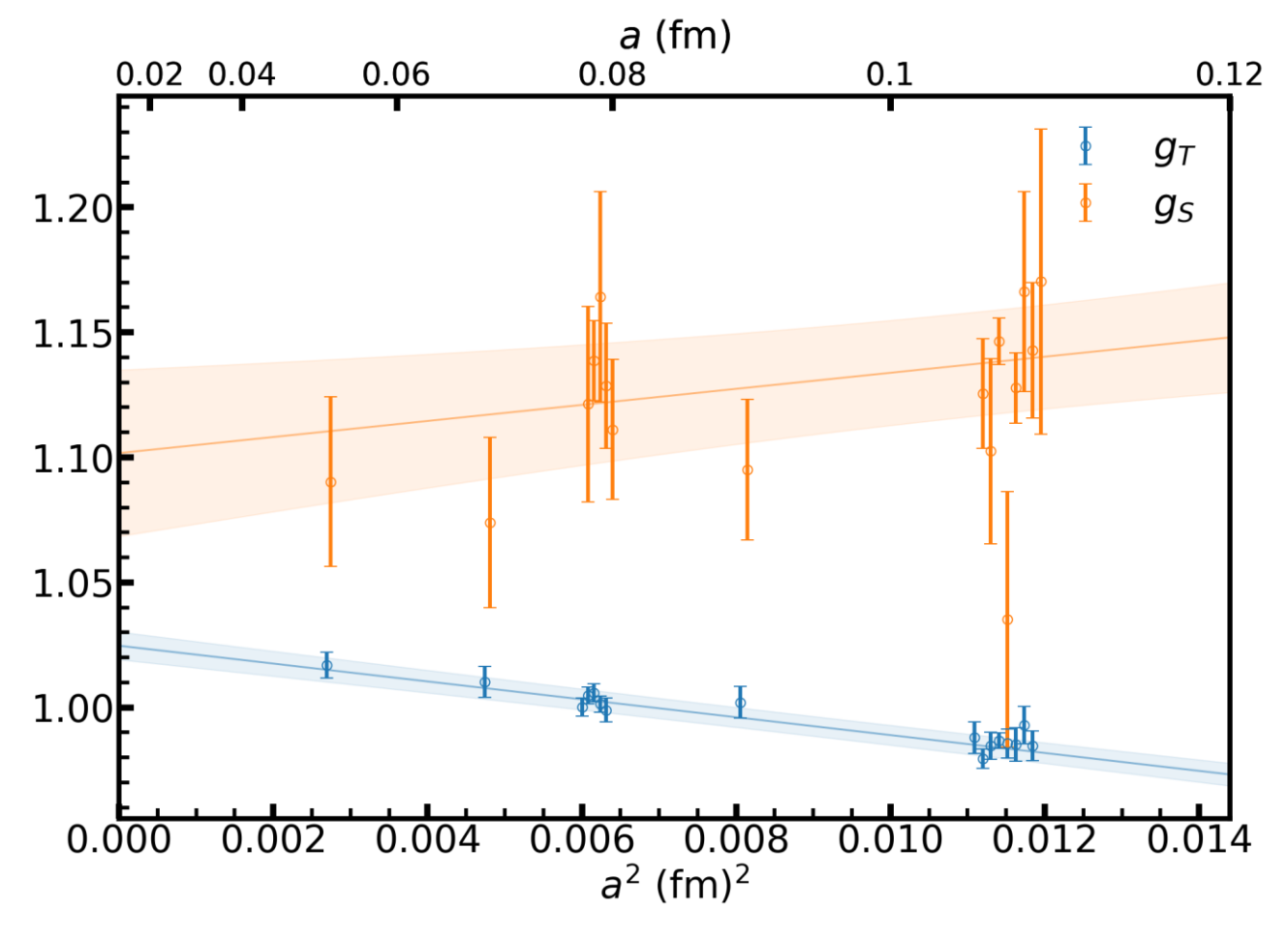
#### Chiral behavior



we can constrain our results at the physical point strongly!

All data point have been corrected to corrected to continuum and infinite volume limits

#### Discretization error

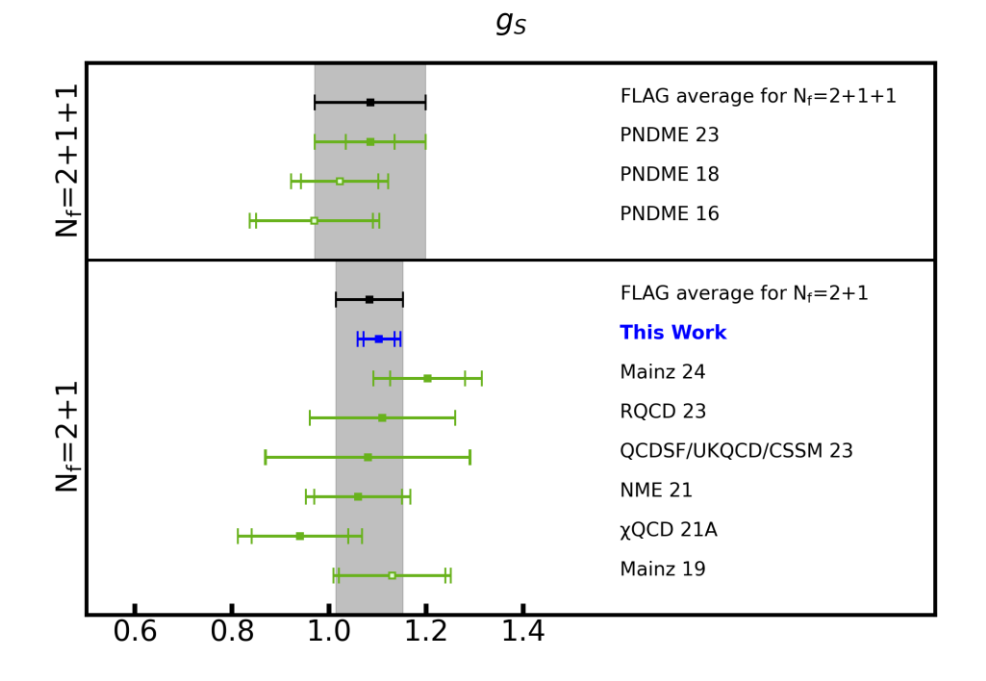


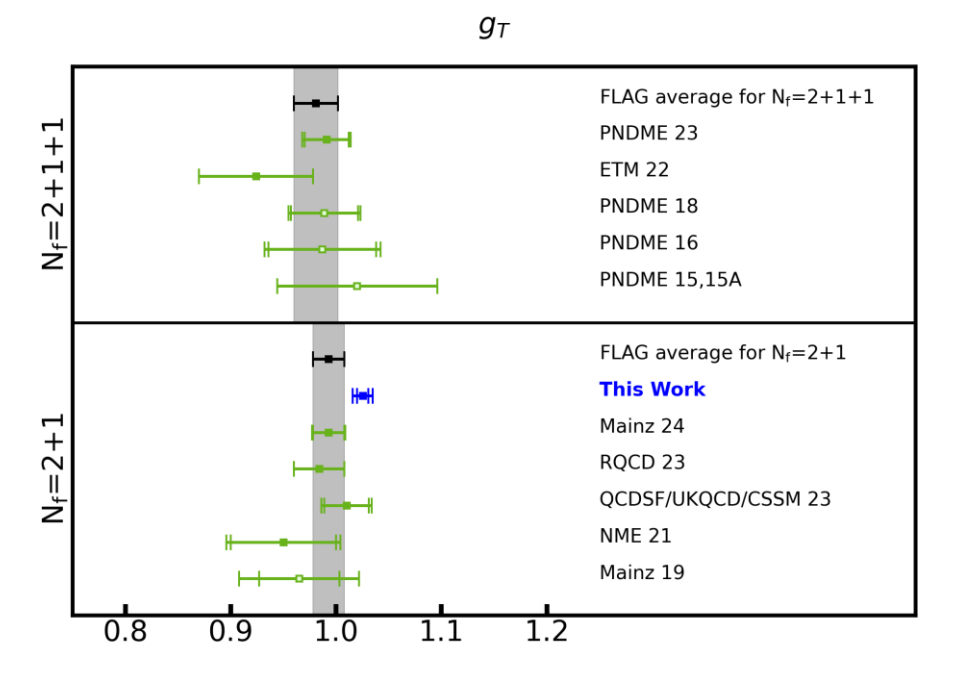
All data point have been corrected to corrected to physical pion mass and infinite volume limits

#### Final Results

The final results of target physical value  $g_X^{\rm QCD}$  are:

$$g_T^{\text{QCD}} = 1.0253[99]_{\text{tot}}(55)_{\text{stat}}(46)_a(59)_{\text{FV}}(13)_{\chi}(34)_{\text{ex}},$$
  
$$g_S^{\text{QCD}} = 1.103[41]_{\text{tot}}(32)_{\text{stat}}(04)_a(26)_{\text{FV}}(01)_{\chi}(01)_{\text{ex}},$$





Our final value has a total uncertainty 1/3 smaller than the current  $N_f$  = 2 + 1 FLAG average

### neutron-proton mass difference

Using  $m_d - m_u$ =2.35(12) MeV[1] (from the FLAG average) and a QED correction of -1.00(7)(14) MeV, we predict the neutron-proton mass difference as

$$m_n - m_p = 1.59[0.23]_{\text{tot}}(0.10)_{g_S}(0.13)_{\text{ISB}}(0.16)_{\text{QED}}.$$

which agrees with the experimental value (1.293 MeV) within  $1.3\sigma$ .

However, using a newer QED correction of -0.58(16) MeV[2] yields a prediction roughly  $3\sigma$  higher than experiment. This discrepance underscores the importance of an up-dated direct lattice QCD+QED calculation of the QED correction.

<sup>[1].</sup> S. Borsanyi et al. (BMW), Science 347, 1452 (2015),arXiv:1406.4088 [hep-lat].

<sup>[2].</sup> J. Gasser, H. Leutwyler, and A. Rusetsky, Phys. Lett. B814, 136087 (2021), arXiv:2003.13612 [hep-ph].

# Summary

- ightharpoonup Our data prefer the form  $e^{-m_{\pi}L}$  over the form  $m_{\pi}^2 e^{-m_{\pi}L}/\sqrt{m_{\pi}L}$  predicted by heavy baryon chiral perturbation theory (HB $\chi$ PT).
- Accurate results on ensembles with physical pion mass allow us to suppress systematic errors arising from model dependence in the treatment of chiral behavior.
- $\triangleright$  We achieve the total uncertainty 1/3 smaller than the current  $N_f$  = 2 + 1 FLAG average